

Single Spin Asymmetries in Charged Pion Production from Semi-Inclusive Deep Inelastic Scattering on a Transversely Polarized ^3He Target at $Q^2 = 1.4 - 2.7 \text{ GeV}^2$

X. Qian,^{1,2,*} K. Allada,³ C. Dutta,³ J. Huang,⁴ J. Katich,⁵ Y. Wang,⁶ Y. Zhang,⁷ K. Aniol,⁸ J.R.M. Annand,⁹ T. Averett,⁵ F. Benmokhtar,¹⁰ W. Bertozzi,⁴ P.C. Bradshaw,⁵ P. Bosted,¹¹ A. Camsonne,¹¹ M. Canan,¹² G.D. Cates,¹³ C. Chen,¹⁴ J.-P. Chen,¹¹ W. Chen,¹ K. Chirapatpimol,¹³ E. Chudakov,¹¹ E. Cisbani,^{15,16} J.C. Cornejo,⁸ F. Cusanno,^{15,16} M. M. Dalton,¹³ W. Deconinck,⁴ C.W. de Jager,¹¹ R. De Leo,¹⁷ X. Deng,¹³ A. Deur,¹¹ H. Ding,¹³ P. A. M. Dolph,¹³ D. Dutta,¹⁸ L. El Fassi,¹⁹ S. Frullani,^{15,16} H. Gao,¹ F. Garibaldi,^{15,16} D. Gaskell,¹¹ S. Gilad,⁴ R. Gilman,^{11,19} O. Glamazdin,²⁰ S. Golge,¹² L. Guo,²¹ D. Hamilton,⁹ O. Hansen,¹¹ D.W. Higinbotham,¹¹ T. Holmstrom,²² M. Huang,¹ H. F. Ibrahim,²³ M. Iodice,²⁴ X. Jiang,^{19,21} G. Jin,¹³ M.K. Jones,¹¹ A. Kelleher,⁵ W. Kim,²⁵ A. Kolarkar,³ W. Korsch,³ J.J. LeRose,¹¹ X. Li,²⁶ Y. Li,²⁶ R. Lindgren,¹³ N. Liyanage,¹³ E. Long,²⁷ H.-J. Lu,²⁸ D.J. Margaziotis,⁸ P. Markowitz,²⁹ S. Marrone,¹⁷ D. McNulty,³⁰ Z.-E. Meziani,³¹ R. Michaels,¹¹ B. Moffit,^{4,11} C. Muñoz Camacho,³² S. Nanda,¹¹ A. Narayan,¹⁸ V. Nelyubin,¹³ B. Norum,¹³ Y. Oh,²⁵ M. Osipenko,³³ D. Parno,¹⁰ J. C. Peng,⁶ S. K. Phillips,³⁴ M. Posik,³¹ A. J. R. Puckett,^{4,13} Y. Qiang,^{1,11} A. Rakhman,³⁵ R. D. Ransome,¹⁹ S. Riordan,¹³ A. Saha,^{11,†} B. Sawatzky,^{31,11} E. Schulte,¹⁹ A. Shahinyan,³⁶ M. H. Shabestari,¹³ S. Širca,³⁷ S. Stepanyan,²⁵ R. Subedi,¹³ V. Sulkosky,^{4,11} L.-G. Tang,¹⁴ A. Tobias,¹³ G. M. Urciuoli,¹⁵ I. Vilardi,¹⁷ K. Wang,¹³ B. Wojtsekhowski,¹¹ X. Yan,²⁸ H. Yao,³¹ Y. Ye,²⁸ Z. Ye,¹⁴ L. Yuan,¹⁴ X. Zhan,⁴ Y.-W. Zhang,⁷ B. Zhao,⁵ X. Zheng,¹³ L. Zhu,^{6,14} X. Zhu,¹ and X. Zong¹

(The Jefferson Lab Hall A Collaboration)

¹Duke University, Durham, NC 27708

²Kellogg Radiation Laboratory, California Institute of Technology, Pasadena, CA 91125

³University of Kentucky, Lexington, KY 40506

⁴Massachusetts Institute of Technology, Cambridge, MA 02139

⁵College of William and Mary, Williamsburg, VA 23187

⁶University of Illinois at Urbana-Champaign, Urbana, IL 61801

⁷Lanzhou University, Lanzhou 730000, Gansu, People's Republic of China

⁸California State University, Los Angeles, Los Angeles, CA 90032

⁹University of Glasgow, Glasgow G12 8QQ, Scotland, United Kingdom

¹⁰Carnegie Mellon University, Pittsburgh, PA 15213

¹¹Thomas Jefferson National Accelerator Facility, Newport News, VA 23606

¹²Old Dominion University, Norfolk, VA 23529

¹³University of Virginia, Charlottesville, VA 22904

¹⁴Hampton University, Hampton, VA 23187

¹⁵INFN, Sezione di Roma, I-00161 Rome, Italy

¹⁶Istituto Superiore di Sanità, I-00161 Rome, Italy

¹⁷INFN, Sezione di Bari and University of Bari, I-70126 Bari, Italy

¹⁸Mississippi State University, MS 39762

¹⁹Rutgers, The State University of New Jersey, Piscataway, NJ 08855

²⁰Kharkov Institute of Physics and Technology, Kharkov 61108, Ukraine

²¹Los Alamos National Laboratory, Los Alamos, NM 87545

²²Longwood University, Farmville, VA 23909

²³Cairo University, Giza 12613, Egypt

²⁴INFN, Sezione di Roma3, I-00146 Rome, Italy

²⁵Kyungpook National University, Taegu 702-701, Republic of Korea

²⁶China Institute of Atomic Energy, Beijing, People's Republic of China

²⁷Kent State University, Kent, OH 44242

²⁸University of Science and Technology of China, Hefei 230026, People's Republic of China

²⁹Florida International University, Miami, FL 33199

³⁰University of Massachusetts, Amherst, MA 01003

³¹Temple University, Philadelphia, PA 19122

³²Université Blaise Pascal/IN2P3, F-63177 Aubière, France

³³INFN, Sezione di Genova, I-16146 Genova, Italy

³⁴University of New Hampshire, Durham, NH 03824

³⁵Syracuse University, Syracuse, NY 13244

³⁶Yerevan Physics Institute, Yerevan 375036, Armenia

³⁷University of Ljubljana, SI-1000 Ljubljana, Slovenia

(Dated: January 26, 2013)

We report the first measurement of target single spin asymmetries in the semi-inclusive ${}^3\text{He}(e, e'\pi^\pm)X$ reaction on a transversely polarized target. The experiment, conducted at Jefferson Lab using a 5.9 GeV electron beam, covers a range of $0.16 < x < 0.35$ with $1.4 < Q^2 < 2.7$ GeV². The Collins and Sivers moments were extracted from the azimuthal angular dependence of the measured asymmetries. The π^\pm Collins moments for ${}^3\text{He}$ are consistent with zero, except for the π^+ moment at $x = 0.35$, which deviates from zero by 2.3σ . While the π^- Sivers moments are consistent with zero, the π^+ Sivers moments favor negative values. The neutron results were extracted using the nucleon effective polarization and measured cross section ratios of proton to ${}^3\text{He}$, and are largely consistent with the predictions of phenomenological fits and quark model calculations.

High-energy lepton-nucleon scattering is a powerful tool to study the partonic structure of the nucleon. While detailed studies of inclusive deep inelastic scattering (DIS) have revealed a great deal of information about the unpolarized (f_1^q) and polarized (g_1^q) parton distribution functions (PDFs) describing the longitudinal momentum and helicity of quarks in the nucleon, understanding of the nucleon's spin structure is far from being complete [1]. In particular, the experimental study of quark transverse spin phenomena has just begun [2–5]. Recent reviews can be found in Ref. [6, 7]. These progresses also point to an important role for quark/gluon orbital angular motion in the nucleon's spin structure. Semi-inclusive DIS (SIDIS), in which a hadron from the fragmentation of the struck quark is detected in coincidence with the scattered lepton, provides access to transverse-momentum-dependent parton distributions (TMDs) [8–10], which describe the quark structure of the nucleon in all three dimensions of momentum space. The ability of SIDIS reactions to access partonic transverse spin and momentum [2, 4, 5, 11–14] relevant to the kinematics of this work provides a unique opportunity for the study of orbital angular momentum (OAM).

All eight leading-twist TMDs are accessible in SIDIS [10]. The angular dependence of the target spin-dependent asymmetry A in the scattering of an unpolarized lepton beam by a transversely polarized target is:

$$A(\phi_h, \phi_S) = \frac{1}{P} \frac{Y_{\phi_h, \phi_S} - Y_{\phi_h, \phi_S + \pi}}{Y_{\phi_h, \phi_S} + Y_{\phi_h, \phi_S + \pi}} \approx A_C \sin(\phi_h + \phi_S) + A_S \sin(\phi_h - \phi_S), \quad (1)$$

where P is the target polarization, ϕ_h and ϕ_S are the azimuthal angles of the hadron momentum and the target spin relative to the lepton scattering plane as defined in the Trento convention [15], Y is the normalized yield, and A_C (A_S) is the Collins (Sivers) moment.

The Collins moment probes the convolution of the chiral-odd quark transversity distribution h_1^q [16] and the chiral-odd Collins fragmentation function (FF) [17]. h_1^q describes the transverse polarization of quarks in a transversely polarized nucleon. Because the gluon transversity vanishes, quark transversity is valence-like [18]. The lowest moment of transversity, the tensor charge, provides a test of lattice QCD predictions [19]. Transversity is further constrained by Soffer's inequality [20], $|h_1^q| \leq \frac{1}{2}(f_1^q + g_1^q)$, which holds under next-to-leading-

order QCD evolution [21–23]. However, a possible violation of Soffer's bound has been suggested [24].

The Sivers moment probes the convolution of the naive T-odd quark Sivers function f_{1T}^\perp [25] and the unpolarized FF. f_{1T}^\perp represents a correlation between the nucleon spin and the quark transverse momentum, and it corresponds to the imaginary part of the interference between light-cone wave function components differing by one unit of OAM [26, 27]. The Sivers function was originally thought to vanish since it is odd under naive time-reversal transformations [17]. A nonzero f_{1T}^\perp was later shown to be allowed due to QCD final state interactions (FSI) between the outgoing quark and the target remnant [26]. It was further demonstrated through gauge invariance that the same Sivers function, which originates from a gauge link, would appear in both SIDIS and Drell-Yan single spin asymmetries (SSAs) but with an opposite sign [28, 29].

The HERMES collaboration carried out the first SSA measurement in SIDIS on a transversely polarized proton target using e^\pm beams [2] at $Q^2 = 1.3 - 6.2$ GeV². The COMPASS collaboration performed SIDIS measurements with a muon beam on transversely polarized deuteron [4] and proton [5] targets at $Q^2 = 1.3 - 20.2$ GeV². Large Collins moments were observed for both π^+ and π^- from the proton, but with opposite sign, indicating that the “unfavored” Collins FF could be as large as the “favored” one [17]. This finding is consistent with the measured asymmetry of inclusive hadron pair production in e^+e^- annihilation from BELLE [30], which directly accessed the product of Collins FFs. The deuteron Collins asymmetries for π^+ and π^- are consistent with zero, but with relatively large uncertainties for $x > 0.1$, which suggests a cancellation between proton and neutron.

While both the HERMES and COMPASS proton data show significantly positive π^+ Sivers moments, a possible inconsistency exists between the data sets [31]. On the other hand, the proton π^- Sivers moments from both HERMES [14] and COMPASS [5] are consistent with zero, along with the COMPASS deuteron π^+ and π^- Sivers moments. These results could reflect pronounced flavor dependence of the Sivers functions, as indicated by a phenomenological fit [31] of these data.

To shed new light on the flavor structures of the transversity and Sivers functions, it is important to extend the SSA SIDIS measurement to a neutron target, which is more sensitive to the nucleon's d quark con-

tribution. Since there is no stable free neutron target, polarized ^3He is commonly used as an effective polarized neutron target [32]. The ^3He nucleus, in which the nuclear spin resides predominantly with the neutron, is uniquely advantageous in the extraction of neutron spin information compared to the deuteron ($p+n$).

In this letter, we present the results of SSA measurements in SIDIS on a transversely polarized ^3He target, performed in Jefferson Lab (JLab) Hall A from 2008/11 to 2009/02. The electron beam energy was 5.9 GeV with an average current of 12 μA . Scattered electrons with momenta from 0.6–2.5 GeV were detected in the BigBite spectrometer at a central angle of 30° on the beam right. Coincident charged hadrons were detected in the High Resolution Spectrometer (HRS) [33] at a central angle of 16° on beam left and a central momentum of 2.35 GeV. Unpolarized beam was achieved by summing the two beam helicity states. The residual beam charge asymmetry was smaller than 100 ppm per 1-hour run.

The 40 cm long polarized ^3He [33] cell was filled at room temperature with ~ 8 atms of ^3He and ~ 0.13 atms of N_2 to reduce depolarization effects. The ^3He nuclei were polarized by Spin Exchange Optical Pumping of a Rb-K mixture. The polarization was monitored by Nuclear Magnetic Resonance (NMR) measurements every 20 minutes as the target spin was automatically flipped through Adiabatic Fast Passage. The NMR measurements were calibrated using the known water NMR signal and cross-checked using the Electron Paramagnetic Resonance method. The average polarization was $55.4 \pm 2.8\%$. Three pairs of mutually orthogonal Helmholtz coils were used to orient the target polarization vertically and horizontally (determined to better than 0.5° using a compass) in the plane transverse to the beam direction in order to maximize the ϕ_S coverage. The holding magnetic field (~ 25 G) remained fixed during spin flips.

The BigBite spectrometer consists of a large-opening dipole magnet in front of a detector stack including three sets of multi-wire drift chambers for charged-particle tracking, a lead-glass calorimeter divided into preshower/shower sections for electron identification and a scintillator plane between the preshower and shower for timing. In this experiment, BigBite was positioned to subtend a solid angle of ~ 64 msr for a 40 cm target. The large out-of-plane angle acceptance of BigBite (± 240 mrad) was essential in maximizing the ϕ_h coverage of the experiment, given the small (~ 6 msr) solid angle acceptance of the hadron arm. The transport matrix of the BigBite magnet was calibrated using a multi-foil carbon target, a sieve slit collimator and $^1\text{H}(e, e')p$ elastic scattering at incident energies of 1.2 and 2.4 GeV. The achieved angular and momentum resolutions were better than 10 mrad and 1%, respectively. Clean e^- identification was achieved using cuts on the preshower energy E_{ps} and the ratio E/p of the total shower energy to the momentum from optics reconstruction. The π^- contami-

nation was determined from analysis of the E_{ps} spectrum to be less than 2%, consistent with GEANT3 simulations.

The HRS detector package was configured for hadron detection [33]. A $10^4:1$ e^- rejection factor was achieved using a light gas Čerenkov and a lead glass calorimeter, resulting in a negligible e^\pm contamination. Coincidence timing provided more than 15σ pion-proton separation. A $10:1$ K^\pm rejection was achieved using the aerogel Čerenkov detector, leaving less than 1% contamination. The $\pm 5\%$ HRS momentum acceptance limited the hadron energy fraction z to about 0.5 (see Table I).

SIDIS events were selected using cuts on the four-momentum transfer squared $Q^2 > 1$ GeV 2 , the hadronic final-state invariant mass $W > 2.3$ GeV, and the mass of undetected final-state particles $W' > 1.6$ GeV, assuming scattering on a nucleon. The total number of accepted SIDIS events are 254k and 194k for π^+ and π^- , respectively. The data were divided into four bins in the Bjorken scaling variable x . The central kinematics of the four bins after radiative corrections are presented in Table I. SIDIS yields were obtained by normalizing the number of identified SIDIS events by the accumulated beam charge and the data acquisition live time. The data were divided into ~ 2850 pairs of measurements in opposite target spin states to extract the raw asymmetries. The false asymmetry due to luminosity fluctuations was confirmed to be less than 4×10^{-4} by measurements of the SSA in inclusive (e, e') scattering with transverse target polarization oriented horizontally, which vanishes due to parity conservation. The raw Collins/Sivers moments were obtained by fitting the asymmetries in 2-D (ϕ_h, ϕ_S) bins according to Eq.(1). This procedure was confirmed by an unbinned maximum-likelihood method. The ^3He moments were obtained after correcting the directly measured N_2 dilution ($\sim 10\%$ contribution).

The dominant background in the SIDIS electron sample comes from e^+/e^- pair production. This background (listed in Table I) was directly measured by reversing the polarity of the BigBite magnet to detect e^+ in identical conditions as e^- . The contamination was treated as a dilution effect in the analysis, as the measured asymmetries were consistent with zero for $e^+-\pi$ coincidence events, which mirror the pair-produced $e^--\pi$ events. Additional experimental uncertainties in the extracted ^3He Collins/Sivers moments include: 1) K^\pm contamination in the π^\pm sample, 2) bin-centering, resolution and radiative effects estimated using simulations, 3) the effect of the target collimator, estimated by varying the scattering vertex cut, 4) target density fluctuations, and 5) the false asymmetry due to yield drift caused by radiation damage to the BigBite preshower calorimeter. The quadrature sum of all above contributions is below 25% of the statistical uncertainty in each x bin.

In addition, there are fitting systematic uncertainties resulting from the neglect of other ϕ_h - and ϕ_S -dependent terms, such as $2\langle \sin(3\phi_h - \phi_S) \rangle$, higher-twist terms in-

x	Q^2 GeV ²	y	z	$P_{h\perp}$ GeV	W GeV	W' GeV	f_{pair}^+	f_{pair}^-	$1 - f_p^+$	$1 - f_p^-$
0.156	1.38	0.81	0.50	0.435	2.91	2.07	22.0±4.4%	24.0±4.8%	0.212 ± 0.032 (0.027)	0.348 ± 0.032 (0.022)
0.206	1.76	0.78	0.52	0.38	2.77	1.97	8.0±2.0%	14.0±2.0%	0.144 ± 0.031 (0.029)	0.205 ± 0.037 (0.027)
0.265	2.16	0.75	0.54	0.32	2.63	1.84	2.5±0.9%	5.0±1.8%	0.171 ± 0.029 (0.028)	0.287 ± 0.036 (0.024)
0.349	2.68	0.70	0.58	0.24	2.43	1.68	1.0±0.5%	2.0±1.0%	0.107 ± 0.026 (0.030)	0.220 ± 0.032 (0.026)

TABLE I. Central kinematics for the four x bins. The fractional e^- energy loss y , the hadron energy fraction z with respect of electron energy transfer and the transverse momentum $P_{h\perp}$ are all defined following the notation of Ref. [10]. The pair production background f_{pair}^{\pm} and the proton dilution $1 - f_p^{\pm}$ are shown with their total experimental systematic uncertainties. The numbers in parentheses represent the model uncertainties corresponding to unpolarized FSI effects.

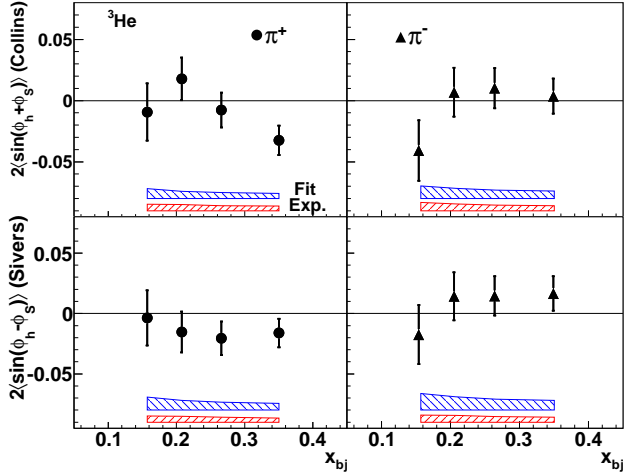


FIG. 1. (Color online) The extracted Collins/Sivers moments on ^3He are shown together with uncertainty bands (see text) for both π^+ and π^- electro-production.

cluding $2\langle\sin\phi_S\rangle$ and $2\langle\sin(2\phi_h - \phi_S)\rangle$, azimuthal modulations of the unpolarized cross section including the Cahn ($2\langle\cos\phi_h\rangle$) and Boer-Mulders ($2\langle\cos(2\phi_h)\rangle$) effects [10], and leakage from the longitudinal SSA (A_{UL}) due to the small longitudinal component of the target polarization. The effects of these terms were estimated by varying each term within an allowed range derived from the HERMES data [34, 35], assuming the magnitude of each term for the neutron is similar to that of the proton. The $2\langle\sin\phi_S\rangle$ term gives the largest effect, followed by the $2\langle\sin(3\phi_h - \phi_S)\rangle$ and $2\langle\sin(2\phi_h - \phi_S)\rangle$ terms.

A Monte Carlo simulation of the experiment was adapted from the package SIMC used in the analysis of SIDIS cross section measurements on ^1H and ^2H from JLab Hall C [12] to include models of our target and spectrometers. SIMC was used to estimate the combined effects of acceptance, resolution and radiative corrections on the extraction of the Collins and Sivers moments, and these effects were included in the experimental systematic uncertainties. Additionally, the contamination in identified SIDIS events from decays of diffractively produced ρ mesons was estimated to range from 3-5% (5-10%) for

π^+ (π^-) by PYTHIA6.4 [36]. Consistent with the HERMES analysis, no corrections for this background have been applied to our results. The contamination from radiative tails of exclusive electroproduction, estimated by normalizing the MC spectrum to the data in the low- W region, was found to be less than 3%.

The extracted ^3He Collins $A_C \equiv 2\langle\sin(\phi_h + \phi_S)\rangle$ and Sivers $A_S \equiv 2\langle\sin(\phi_h - \phi_S)\rangle$ moments are shown in Fig. 1 and tabulated in Table. II. The error bars represent statistical uncertainties only. The experimental systematic uncertainties combined in quadrature are shown as the band labeled “Exp.”. The combined extraction model uncertainties due to neglecting other allowed terms are shown as the band labeled “Fit”. The extracted ^3He Collins and Sivers moments are all below 5%. The Collins moments are mostly consistent with zero, except the π^+ Collins moment at $x=0.35$, which deviates from zero by 2.3σ after combining the statistical and systematic uncertainties in quadrature. The π^+ Sivers moments favor negative values, and the π^- Sivers moments are consistent with zero.

To extract the neutron Collins/Sivers SSAs ($A_n^{C/S}$) from the measured ^3He moments ($A_{^3\text{He}}^{C/S}$), we used,

$$A_{^3\text{He}}^{C/S} = P_n \cdot (1 - f_p) \cdot A_n^{C/S} + P_p f_p \cdot A_p^{C/S}, \quad (2)$$

which was shown to be valid in a calculation by Scopetta [37] including initial-state nuclear effects. Here, $P_n = 0.86^{+0.036}_{-0.02}$ ($P_p = -0.028^{+0.009}_{-0.004}$) is the neutron (proton) effective polarization [38]. The proton dilution $f_p = \frac{2\sigma_p}{\sigma_{^3\text{He}}}$ of ^3He was measured by comparing the yields of unpolarized hydrogen and ^3He targets in the SIDIS kinematics. An additional model uncertainty from spin-independent FSI was estimated using pion multiplicity data [39] and a Lund string model-based calculation of the pion absorption probability [40]. An upper limit of 3.5% on the size of the FSI effect was used to estimate the uncertainty in f_p , shown in Table I, and included in the “Fit” systematic uncertainty. The neutron SSAs due to spin-dependent FSI were estimated to be well below 1% across the entire x range with a simple Glauber rescattering model.

The resulting neutron Collins/Sivers moments calculated using Eq. (2), with f_p from our data and proton Collins/Sivers moments from Refs. [41–43], are shown in

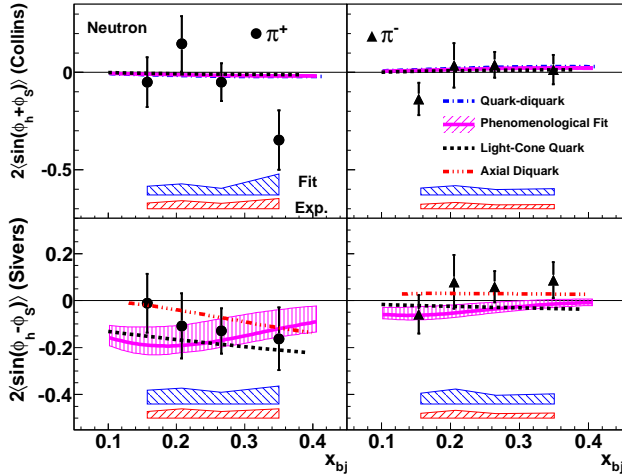


FIG. 2. (Color online) The extracted neutron Collins and Sivers moments with uncertainty bands for both π^+ and π^- electro-production. See text for details.

Fig. 2 and tabulated in Table. II. Corrections from the proton Collins/Sivers moments are less than 0.012. Our Collins moments are compared with the phenomenological fit [42], a light-cone quark model calculation [44, 45] and quark-diquark model [46, 47] calculations. The phenomenological fit and the model calculations, which assume Soffer's bound [20], predict rather small Collins asymmetries which are mostly consistent with our data. However, the π^+ Collins moment at $x = 0.34$ is suggestive of a noticeably more negative value at the 2σ level. Our data favor negative π^+ Sivers moments, while the π^- moments are close to zero. Such behavior independently supports a negative d quark Sivers function within the parton model picture, which has been suggested by predictions of the phenomenological fit [41, 43] to HERMES and COMPASS data, a light-cone quark model calculation [48, 49], and an axial diquark model calculation [50].

In summary, we have reported the first measurement of the SSA in charged pion electroproduction on a transversely polarized ^3He target in the DIS region. Our data provide the best current measurement of the neutron Sivers moments in the valence region ($x > 0.1$), and the best neutron Collins moments for $x > 0.2$, which will further improve the extraction of d quark distributions in these regions. This experiment has demonstrated the power of polarized ^3He as an effective polarized neutron target, and has laid the foundation for future high-precision measurements of TMDs with a large acceptance detector SoLID following the JLab 12 GeV upgrade [51] and at an electron-ion collider [52]. These future SIDIS data taken over a broad range of Q^2 will also allow an accurate determination of higher twist contribution [53, 54].

We acknowledge the outstanding support of the JLab

Hall A technical staff and the Accelerator Division in accomplishing this experiment. This work was supported in part by the U. S. National Science Foundation, and by DOE contract number DE-AC05-06OR23177, under which the Jefferson Science Associates (JSA) operates the Thomas Jefferson National Accelerator Facility.

* Corresponding author: xqian@caltech.edu

† Deceased

- [1] S. E. Kuhn *et al.*, Prog. Part. Nucl. Phys. **63**, 1 (2009).
- [2] A. Airapetian *et al.*, Phys. Rev. Lett. **94**, 012002 (2005).
- [3] A. Airapetian *et al.*, Phys. Lett. B **693**, 11 (2010).
- [4] M. Alekseev *et al.*, Phys. Lett. **B673**, 127 (2009).
- [5] M. Alekseev *et al.*, Phys. Lett. **B692**, 240 (2010).
- [6] V. Barone *et al.*, Phys. Rept. **359**, 1 (2002).
- [7] V. Barone *et al.*, Prog. Part. Nucl. Phys. **65**, 267 (2010).
- [8] P. J. Mulders and R. D. Tangerman, Nucl. Phys. **B461**, 197 (1996).
- [9] D. Boer and P. Mulders, Phys. Rev. **D57**, 5780 (1998).
- [10] A. Bacchetta *et al.*, JHEP **02**, 093 (2007).
- [11] X. D. Ji *et al.*, Phys. Rev. **D71**, 034005 (2005).
- [12] R. Asaturyan *et al.*, (2011), arXiv:1103.1649.
- [13] H. Avakian *et al.*, Phys. Rev. **D69**, 112004 (2004).
- [14] A. Airapetian *et al.*, Phys. Rev. Lett. **103**, 152002 (2009).
- [15] A. Bacchetta *et al.*, Phys. Rev. **D70**, 117504 (2004).
- [16] J. P. Ralston and D. E. Soper, Nucl. Phys. **B152**, 109 (1979).
- [17] J. C. Collins, Nucl. Phys. **B396**, 161 (1993).
- [18] C. Bourrely *et al.*, Phys. Lett. **B420**, 375 (1998).
- [19] M. Gockeler *et al.*, Phys. Lett. **B627**, 113 (2005).
- [20] J. Soffer, Phys. Rev. Lett. **74**, 1292 (1995).
- [21] S. Kumano and M. Miyama, Phys. Rev. **D56**, 2504 (1997).
- [22] A. Hayashigaki *et al.*, Phys. Rev. **D56**, 7350 (1997).
- [23] W. Vogelsang, Phys. Rev. **D57**, 1886 (1998).
- [24] J. P. Ralston, (2008), arXiv:0810.0871.
- [25] D. Sivers, Phys. Rev. **D41**, 83 (1990).
- [26] S. J. Brodsky *et al.*, Phys. Lett. **B530**, 99 (2002).
- [27] X. D. Ji *et al.*, Nucl. Phys. **B652**, 383 (2003).
- [28] J. C. Collins, Phys. Lett. **B536**, 43 (2002).
- [29] S. J. Brodsky *et al.*, Nucl. Phys. **B642**, 344 (2002).
- [30] R. Seidl *et al.*, Phys. Rev. Lett. **96**, 232002 (2006).
- [31] M. Anselmino *et al.*, (2010), arXiv:1012.3565.
- [32] F. Bissey *et al.*, Phys. Rev. **C65**, 064317 (2002).
- [33] J. Alcorn *et al.*, Nucl. Instr. and Meth. **A522**, 294 (2004).
- [34] M. Diefenthaler, Ph.D. Desy-thesis-10-032 (2010).
- [35] R. M. Lamb, Ph.D. Thesis, UIUC (2010).
- [36] T. Sjöstrand *et al.*, JHEP **05**, 026 (2006).
- [37] S. Scopetta, Phys. Rev. **D75**, 054005 (2007).
- [38] X. Zheng *et al.*, Phys. Rev. **C70**, 065207 (2004).
- [39] A. Airapetian *et al.*, Nucl. Phys. **B780**, 1 (2007).
- [40] A. Accardi *et al.*, Nucl. Phys. **A720**, 131 (2003).
- [41] M. Anselmino *et al.*, Phys. Rev. **D72**, 094007 (2005).
- [42] M. Anselmino *et al.*, Phys. Rev. **D75**, 054032 (2007).
- [43] M. Anselmino *et al.*, (2008), arXiv:0812.4366.
- [44] S. Boffi *et al.*, Phys. Rev. **D79**, 094012 (2009).
- [45] B. Pasquini *et al.*, Phys. Rev. **D78**, 034025 (2008).
- [46] J. She and B. Q. Ma, Phys. Rev. **D83**, 037502 (2011).
- [47] B. Q. Ma *et al.*, Phys. Rev. **D65**, 034010 (2002).
- [48] S. Arnold *et al.*, (2008), arXiv:0805.2137.

	x_{bj}	Collins Moment π^+	Collins Moment π^-	Sivers Moment π^+	Sivers Moment π^-
^3He	0.156	$-0.009 \pm 0.023 \pm 0.005$ (0.008)	$-0.041 \pm 0.025 \pm 0.007$ (0.010)	$-0.004 \pm 0.023 \pm 0.005$ (0.011)	$-0.017 \pm 0.025 \pm 0.006$ (0.014)
^3He	0.206	$0.018 \pm 0.017 \pm 0.005$ (0.006)	$0.007 \pm 0.020 \pm 0.006$ (0.008)	$-0.015 \pm 0.017 \pm 0.005$ (0.008)	$0.014 \pm 0.020 \pm 0.006$ (0.011)
^3He	0.265	$-0.008 \pm 0.014 \pm 0.004$ (0.005)	$0.010 \pm 0.016 \pm 0.005$ (0.007)	$-0.021 \pm 0.014 \pm 0.004$ (0.006)	$0.015 \pm 0.016 \pm 0.005$ (0.009)
^3He	0.349	$-0.033 \pm 0.012 \pm 0.004$ (0.004)	$0.004 \pm 0.014 \pm 0.004$ (0.006)	$-0.016 \pm 0.012 \pm 0.003$ (0.006)	$0.017 \pm 0.014 \pm 0.004$ (0.008)
n	0.156	$-0.050 \pm 0.128 \pm 0.029$ (0.044)	$-0.137 \pm 0.084 \pm 0.023$ (0.036)	$-0.011 \pm 0.125 \pm 0.028$ (0.059)	$-0.059 \pm 0.082 \pm 0.019$ (0.046)
n	0.206	$0.146 \pm 0.143 \pm 0.041$ (0.057)	$0.036 \pm 0.114 \pm 0.032$ (0.048)	$-0.108 \pm 0.138 \pm 0.039$ (0.068)	$0.080 \pm 0.114 \pm 0.033$ (0.064)
n	0.265	$-0.050 \pm 0.097 \pm 0.027$ (0.034)	$0.039 \pm 0.067 \pm 0.019$ (0.028)	$-0.129 \pm 0.096 \pm 0.028$ (0.049)	$0.059 \pm 0.067 \pm 0.019$ (0.037)
n	0.349	$-0.348 \pm 0.153 \pm 0.051$ (0.109)	$0.015 \pm 0.076 \pm 0.021$ (0.032)	$-0.163 \pm 0.133 \pm 0.039$ (0.076)	$0.087 \pm 0.077 \pm 0.022$ (0.044)

TABLE II. Tabulated results. Format follows “central value” \pm “statistical uncertainty” \pm “experimental systematic uncertainty” (“model systematic uncertainties”).

- [49] B. Pasquini and P. Schweitzer, (2011), arXiv:1103.5977. [53] E. Leader *et al.*, Phys. Rev. **D75**, 074027 (2007).
[50] L. P. Gamberg *et al.*, Phys. Rev. **D77**, 094016 (2008). [54] J. Blümlein and H. Böttcher, (2011), arXiv:1005.3113.
[51] H. Gao *et al.*, Eur. Phys. J. **Plus** **126**, 2 (2011).
[52] M. Anselmino *et al.*, Eur. Phys. J. **A47**, 35 (2011).